

Use of CR-39 detectors to determine the branching ratio in Pd/D co-deposition

P. A. Mosier-Boss^{1,*}, L. P. Forsley², A. S. Roussetski³, A. G. Lipson⁴,
F. Tanzella⁵, E. I. Saunin⁴, M. McKubre⁵, B. Earle⁵ and D. Zhou⁶

¹9112 Fermi Ave. San Diego, CA, USA

²JWK Corp., 5101B Backlick Road, Annandale, VA 22003, USA

³P.N. Lebedev Physics Institute of Russian Academy of Sciences, Moscow 119991, Russia

⁴A. N. Frumkin Institute of Physical Chemistry and Electrochemistry, Russian Academy of Sciences, Moscow 119991, Russia

⁵SRI International, Menlo Park, CA 94025, USA

⁶National Space Science Center, Chinese Academy of Sciences, Beijing 10019

Columbia Resin-39 (CR-39) detectors used in Pd/D co-deposition experiments were examined using an optical microscope, scanned using an automated scanner, and underwent both sequential etching analysis as well as LET spectrum analysis. These analyses identified and quantified the energetic particles responsible for the tracks observed in the CR-39 detectors and made it possible to estimate the branching ratios of the primary and secondary reactions.

Keywords: Branching ratio, protons, fission, long-range alphas, neutrons.

Introduction

CR-39 detectors were used in Pd/D co-deposition experiments. During the experiments, the detectors were in close proximity to the cathode. After etching, the detectors were analysed by three techniques that gave complementary results. From these analyses, the branching ratios of the primary and secondary reactions were estimated.

Results and discussion

Several Pd/D co-deposition experiments that used Columbia Resin-39 (CR-39; Fukuvi), a solid-state nuclear track detector commonly used to detect energetic particles, were conducted in the presence of an external magnetic field. Two experiments were done with the detector, in contact with the cathode, inside the cell. A 60 μm thick polyethylene film separated the Ag cathode from the detector. These detectors, identified as 10-5 and 10-6, underwent microscopic examination. Figure 1 *a* shows a representative photomicrograph of tracks observed on the front side of the detector. This is the side of the detector that was in contact with the cathode. A control experiment that was done using a CR-39 detector with a 60 μm thick

polyethylene cover and electroplating using CuCl_2 instead of PdCl_2 . For both CuCl_2 and PdCl_2 , the same electrochemical reactions occur at the anode and cathode. Specifically, oxygen and chlorine gas evolution occurs at the anode while deuterium gas evolution and metal electroplating occur at the cathode. In addition, the resultant Cu and Pd metallic deposits exhibit similar dendritic morphologies. The only significant difference is that Pd absorbs deuterium while Cu does not. No tracks were observed for the CuCl_2 experiment. This indicates that the tracks observed in the PdCl_2 experiment are not due to either chemical or mechanical damage of the CR-39 detector.

After microscopic examination, detectors 10-5 and 10-6 were scanned using a TASL automated scanning track analysis system to obtain quantitative information on the pits produced in CR-39. The images were taken at a resolution of 0.8 $\mu\text{m}/\text{pixel}$. The scanner makes 15 characteristic measurements of each feature located in the image. These measurements include track length and diameter, optical density (average image contrast) and symmetry. The scanner then applies image analysis algorithms on these measurements to discriminate between etched tracks and background features. The scanner detected and measured tracks on both sides of the detectors. [Figure S1 \(see Supplementary Information online\)](#) shows the spatial distribution of the tracks on CR-39 detector 10-5. The tracks are denser where the Pd deposits were in contact with the detector, indicating that Pd is the source of the tracks. Figure 1 *b* and *c* shows the results of those scans obtained for both sides of detector 10-5. There are a greater number of tracks on the front side, which is in contact with the cathode. [Figure S2 \(see Supplementary Information online\)](#) shows the results of scanning a blank CR-39 detector. The number of tracks in the blank detector is more than two orders of magnitude less than the number of tracks in detector 10-5. Also, the size distribution of tracks in the blank detector is significantly different than that obtained for detector 10-5.

The scanned data of detectors 10-5 and 10-6 were then subjected to a linear energy transfer (LET) spectrum

*For correspondence. (e-mail: pboss@san.rr.com)

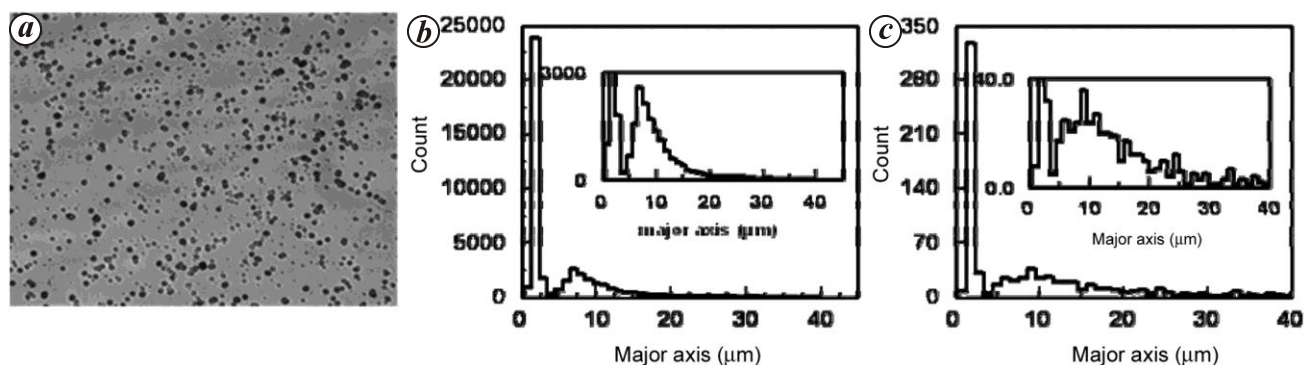


Figure 1. *a*, Photomicrograph of CR-39 detector 10-5 obtained at 200 \times magnification. The detector had been etched in 6.5 N NaOH at 65 $^{\circ}$ C for 7 h. *b*, *c*, Scanned results obtained for CR-39 detector 10-5: *b*, for the front surface (34,254 tracks) and *c*, for the back surface (750 tracks).

analysis^{1,2}. The results of the LET spectrum analysis for both sides (front and back) of detectors 10-5 and 10-6, summarized in [Figure S3 \(see Supplementary Information online\)](#), are similar. The LET spectrum analysis identified tracks on the back side as being either 0–9 MeV protons or 2–15 MeV alphas. It is unlikely that the tracks attributed to 2–15 MeV alphas are actually caused by alphas. In order to pass through a 1 mm thick CR-39 detector, the alpha particles must have energies ≥ 40 MeV. Instead, these tracks are caused by another energetic particle whose tracks resemble those created by 2–15 MeV alphas. The most likely particles responsible for these tracks are neutrons. With regard to the tracks on the back side identified as 0–9 MeV protons, protons with energies >11 MeV will be able to traverse through 1 mm thick CR-39 and 60 μm polyethylene. Consequently, the tracks identified as being due to 9 MeV are actually >11 MeV protons that have gone through both the detector and polyethylene film. The tracks between 0 and 9 MeV are attributed to proton recoil caused by neutrons. Phillips *et al.*³ showed that 2.45 MeV neutrons produce tracks of the same size and shape as those created by <15 MeV alphas and <9 MeV protons.

The observation of triple tracks in CR-39 detectors provides additional evidence of neutron emissions in the Pd/D co-deposition system. Triple tracks are diagnostic of the $^{12}\text{C}(n, n')3\alpha$ carbon break-up reaction^{4,5}. For this reaction to occur in CR-39, the neutron needs to have an energy ≥ 9.6 MeV. [Figure S4 a \(see Supplementary Information online\)](#), shows tracks in a region on detector 10-5 where the track density is low. The circled object in [Figure S4 a](#) is a triple track as shown by taking images of the object at different focusing depths ([Figure S4 b](#)). When the microscope optics were focused on the surface of the detector, the image showed an object comprised of a dark circular pit at the centre with two light-coloured side lobes. An overlay of two images taken at two focusing depths (surface of the detector and bottom of the pits), showed that the two side lobes were breaking away from a centre point. These features are diagnostic of

triple tracks, as shown by the DT generated triple track shown ([Figure S4 c](#)). Microscopic examination of blank detectors has not shown the presence of triple tracks.

Neutron emissions were also observed in a Pd/D co-deposition experiment in which the CR-39 detector was placed outside the cell. A 6 μm thick Mylar film separated the Ag cathode from the detector. Upon completion of the experiment, the detector underwent sequential etching analysis⁶. [Figure S5 a \(see Supplementary Information online\)](#), shows the reconstruction of the proton recoil spectrum for the CR-39 detector used in that experiment after 14 h of etching. The energy of the neutrons is centred on 2.45 MeV.

The LET spectrum analysis of the detectors 10-5 and 10-6 identified the tracks on the front side as being either 2–15 MeV alphas or 2–14 MeV protons ([Figure S3 a](#)). As indicated *vide supra*, the front side of these detectors was in direct contact with the cathode. Both detectors were covered with 60 μm thick polyethylene films throughout the course of the experiments. The energies shown in [Figure S3 a](#) take into account the effect of the 60 μm thick polyethylene film between the cathode and the detector on the particle energies. In the figure there is a peak in the proton energy at 3 MeV. Protons with energies of 3 MeV will go through the 60 μm thick polyethylene film to reach the detector. In contrast, 1 MeV tritons, 0.82 MeV ^3He , and <7 MeV alphas cannot pass through the 60 μm thick polyethylene film and will not leave a track in the detector. As shown in [Figure S5 b](#), sequential etching analysis⁶ also identified 3 MeV protons.

The energetic particles detected by the CR-39 detectors can be born anywhere within the Pd deposit. These particles lose energy as they traverse through the Pd deposit, water film and polyethylene film before they impact the detector. Consequently, the particles identified as >3.4 MeV protons in [Figure S1 a](#) are actually due to protons with much greater energies (~ 12 – 17 MeV). The same is true of the particles identified as alphas in [Figure S1 a](#). These alpha particles, when they were born, have greater energies (~ 12 – 16 MeV). The sequential etching

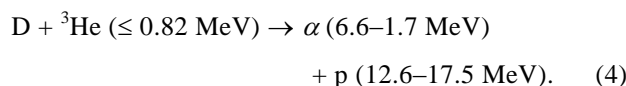
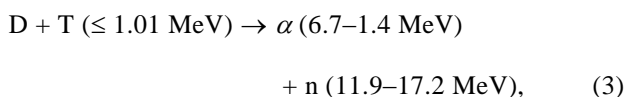
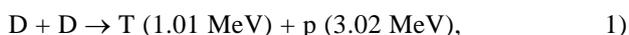
Table 1. Summary of the CR-39 track data for detectors 10-5 and 10-6 used to estimate the branching ratio

Reagents	Reaction products	
D + D	T (1.01 MeV) blocked	p (3.02 MeV) # tracks = 9,873 Correction factor > 133 # of protons > 1.32×10^6
D + D	^3He (0.82 MeV) blocked	n (2.45 MeV) # tracks = 643 (back side) Corrected # tracks = 1,286 ϵ_{DD} (ref. 14) = 1.3×10^{-4} # of neutrons = 9.9×10^6
D + T	α (6.7–1.4 MeV) blocked	n (11.9–17.5 MeV) # triple tracks = 2 ϵ_{DT} (ref. 14) = 5.0×10^{-5} $\epsilon_{\text{triple tracks}}$ = 3.38% # of neutrons = 1.18×10^6
D + ^3He	α (6.6–1.7 MeV) blocked	p (12.6–17.5 MeV) # tracks = 51,734 Correction factor = 6.3 to 5.4 # of protons = 2.29×10^5 to 3.26×10^5

analysis⁶ also identified 12 and 16 MeV alpha particles, as shown in Figure S5 b.

Since these very energetic protons and alphas lose energy as they move through the Pd deposit, water film and polyethylene film, it is expected that CR-39 will register a continuum of energies. This is true of the alpha particles. As can be seen in Figure S3 a, for the >3.4 MeV protons, gaps are observed for proton energies of 6, 11, and 13 MeV. These gaps suggest that protons of these energies are being consumed. Recently, the activation cross-sections of proton-induced nuclear reactions have been measured for Pd^{7,8}. For $^{110}\text{Pd}(p, n\gamma)^{110}\text{Ag}$ reactions at proton energies between 6.0 and 7.7 MeV, activation cross-sections ranged between 100 and 400 mbarn (ref. 8). It is therefore conceivable that these proton reactions on Pd are responsible for the observed loss in protons at 6, 11 and 13 MeV. The Ag isotopes formed from these proton-induced nuclear reactions either stay as Ag or they decay to Pd or Cd. Dash and co-workers^{9,10} have observed Ag and Cd in the SEM/EDX analysis of bulk Pd cathodes as well as Pd/D co-deposition.

The majority of the energetic particles identified by microscopic analysis, sequential etching and LET spectrum analysis can be accounted for by the following primary, (1 and 2) and secondary (3 and 4) nuclear reactions



The results of the LET spectrum analysis (Figure S3), differentiated and quantified the particles generated. These numbers were then used to estimate the branching ratios of the primary and secondary reactions. The presence of the 60 μm polyethylene film between the cathode and the CR-39 detector simplified the analysis as the film prevents 1.01 MeV tritons, 0.82 MeV ^3He , and 1.4–6.7 MeV alphas from reaching the detector. The remaining particles in reactions (1)–(4), the protons and neutrons, will produce visible tracks in the detector.

Table 1 summarizes the identity of the particles causing the tracks in detectors 10-5 and 10-6 as well as the number of tracks attributed to those species which were obtained from the LET spectrum analysis. The number of tracks for 3.02 MeV protons and 12.6–17.5 MeV protons is underestimated due to the fact that these protons are produced throughout the Pd deposit and in all directions. Not all of these protons will reach the CR-39 detector and leave an etchable ionization trail. To correct for this, TRIM (transport of ions in matter) calculations were done¹¹. TRIM is a Monte-Carlo calculation which follows the ion into the target, making detailed calculations of the energy transferred to every target atom collision. The resultant correction factors are tabulated as well as the estimated number of protons.

The number of tracks on the back side due to 2.45 MeV neutrons are also tabulated in Table 1. As neutron interactions with CR-39 occur throughout the detector, the number of neutron generated tracks on the front

side is nearly equal to that on the back side. Consequently, the total number of neutron-generated tracks for both detectors is double that on the back side (Table 1). The efficiency of CR-39 detectors for DD neutrons, ϵ_{DD} , is also tabulated. This efficiency is then used to calculate the total number of DD neutrons shown in Table 1.

For both detectors, two triple tracks were identified. This number is given in Table 1, along with the DT neutron efficiency, ϵ_{DT} , to cause tracks in CR-39. However, this efficiency includes the H, C, and O recoils as well as the carbon break-up reaction. To determine the efficiency for producing triple tracks, a CR-39 detector was exposed to DT neutrons. After etching, the singular and triple tracks were counted. It was found that 3.4% of the DT-generated tracks were triple tracks, the $\epsilon_{\text{triple track}}$ (Table 1). Both of these efficiencies were used to calculate the total number of DT neutrons shown in Table 1.

From the data summarized in Table 1, it is possible to estimate the n/p branching ratios of the primary and secondary reactions. For the primary reactions, the n/p ratio is estimated to be 7.5. This is the maximum value for the branching ratio as the number of 3.02 MeV protons is underestimated. For the secondary reactions, the n/p ratio is estimated to be 5.2–3.6. Again, this is the maximum value for the branching ratio as the number of 12.6–17.5 MeV protons is also underestimated.

The primary and secondary reactions do not account for alphas with energies ≥ 12 MeV. The most common source of such energetic alphas is ternary fission¹². Fission could explain the origins of the new elements that have been reported for Pd/D co-deposition experiments as many of these new elements have masses approximately half that of Pd^{9,10,13}.

Conclusions

Three different analysis techniques were used to analyse CR-39 detectors used in Pd/D co-deposition experiments.

These gave complementary results and made it possible to estimate the branching ratios of the primary and secondary nuclear reactions. They also provided evidence of additional reactions that result in the formation of new elements.

1. O'Sullivan, D. *et al.*, Cosmic rays and dosimetry at aviation altitudes. *Radiat. Meas.*, 1999, **31**, 579–584.
2. Zhou, D. *et al.*, Radiation measured for ISS-Expedition 12 with different dosimeters. *Nucl. Instrum. Methods A*, 2007, **580**, 1283–1289.
3. Phillips, G. W. *et al.*, Neutron spectrometry using CR-39 track etch detectors. *Radiat. Prot. Dosim.*, 2006, **120**, 457.
4. Al-Najjar, S. A. R., Abdel-Naby, A. and Durrani, S. A., Fast-neutron spectrometry using the triple- α reaction in the CR-39 detector. *Nucl. Tracks Radiat. Meas.*, 1986, **12**, 611–615.
5. Abdel-Moneim, A. M. and Abdel-Naby, A., A study of fast neutron beam geometry and energy distribution using triple- α reactions. *Radiat. Meas.*, 2003, **37**, 15–19.
6. Roussetski, A. S. *et al.*, Correct identification of energetic alpha and proton tracks in experiments on CR-39 charged particle detection during hydrogen desorption from Pd/PdO:Hx heterostructure. In Proceedings of the Twelfth International Conference on Condensed Matter Nuclear Science, Yokohama, Japan, 2005.
7. Ditró, F. *et al.*, Measurement of activation cross sections of the proton induced nuclear reactions on palladium. *J. Radioanal. Nucl. Chem.*, 2007, **272**, 231–235.
8. Bi-Tao, H., Zarubin, P. P. and Juravlev, U. U., $^{106,110}\text{Pd}(p, n\gamma)\text{Ag}^{106,110}$ reactions at $E_p = 6.0\text{--}7.7$ MeV. *Chin. Phys.*, 2007, **16**, 989–993.
9. Dash, J. and Miguét, S., Microanalysis of palladium after electrolysis in heavy water. *J. New Energy*, 1996, **1**, 23–27.
10. Dash, J. and Ambadkar, A., Co-deposition of palladium with hydrogen isotopes. In Proceedings of the Eleventh International Conference on Condensed Matter Nuclear Science, Marseille, France, 2004.
11. Ziegler, J. F. and Biersack, J. P., *The Stopping and Range of Ions in Solids*, Pergamon, New York, 1985.
12. https://en.wikipedia.org/wiki/Ternary_fission
13. Szpak, S., Mosier-Boss, P. A., Young, C. and Gordon, F. E., Evidence of nuclear reactions in the Pd lattice. *Naturwissenschaften*, 2005, **92**, 394–397.
14. Collopy, M. T. *et al.*, Calibration of CR-39 for detecting fusion neutrons. *Rev. Sci. Instrum.*, 1992, **63**, 4892–4894.